Synthesis of diamond from gas phase:
technique, properties and applications

В.Г. Ральченко

Институт общей физики им. А.М. Прохорова РАН,
Москва, ralchenko@nsc.gpi.ru

Properties of diamond

Property	Value	Application
Band gap, eV	**5.4**	**High-temperature electronics**
Carrier mobility, cm^2/Vs	**1600 *h* 2200 *e***	**Radiation-hard detectors Optoelectronic switches**
Resistivity, Ohm*cm	**10^{13}-10^{15}**	
Thermal conductivity, W/mK	**2000-2400**	**Heat sinks**
Dielectric constant	**5.7**	
Loss tangent @170 GHz	**$0.3\cdot10^{-6}$**	**Windows for gyrotrons, klystrons**
Optical transmission range	**225 nm – RF**	**Optics for lasers (mostly IR)**
Hardness, GPa	**81±18**	**Tools, surgery blades**
Acoustic wave velocity, km/s	**18.4 *along <111>***	**Surface acoustic wave devices**
Thermal expansion coefficient, 10^{-6} K^{-1}	**0.8 @293 K**	**Stable-dimension components**
Corrosion resistance	**Stable in HF**	**Electrochemistry (doped diamond)**
Low or negative electron affinity		**Field electron emitters**
Biocompatibility		**Coatings on implants**

Atomic structure of diamond

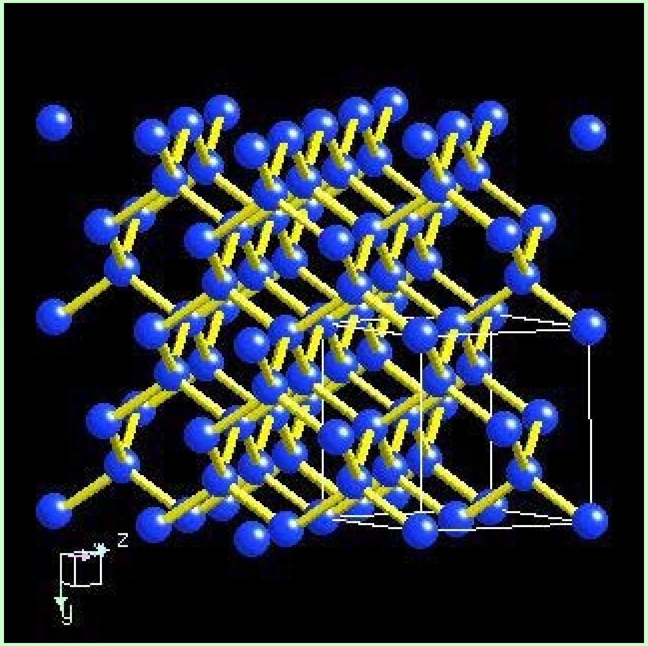

- atomic density 1.76×10^{23} cm^{-3} (record high)
- lattice parameter a=3.56 A
- interatomic distance 1.54 A

Remarkable properties of diamond are result of
- light atom (Z=6)
- short and strong covalent bonding.

Debye temperature T_D = 1860 K
→ T=300 K is low temperature for diamond.

Displacement energy of atom from lattice ≈30 eV
→ radiation hardness.

Single crystal diamonds

Natural stones

- small size
- uncontrolled impurities and defects.

Artificial crystals.

Synthesis at high pressures P=5GPa, T=1600K

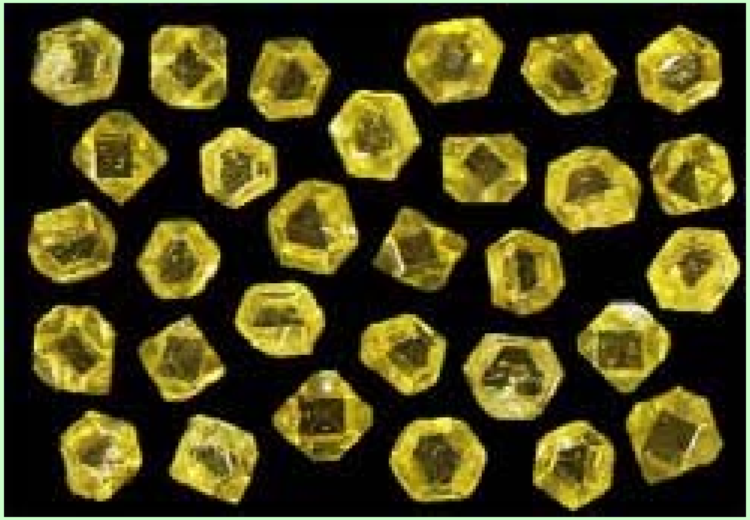

- small size – few mm.
- catalyst impurities.

Polycrystalline CVD diamond

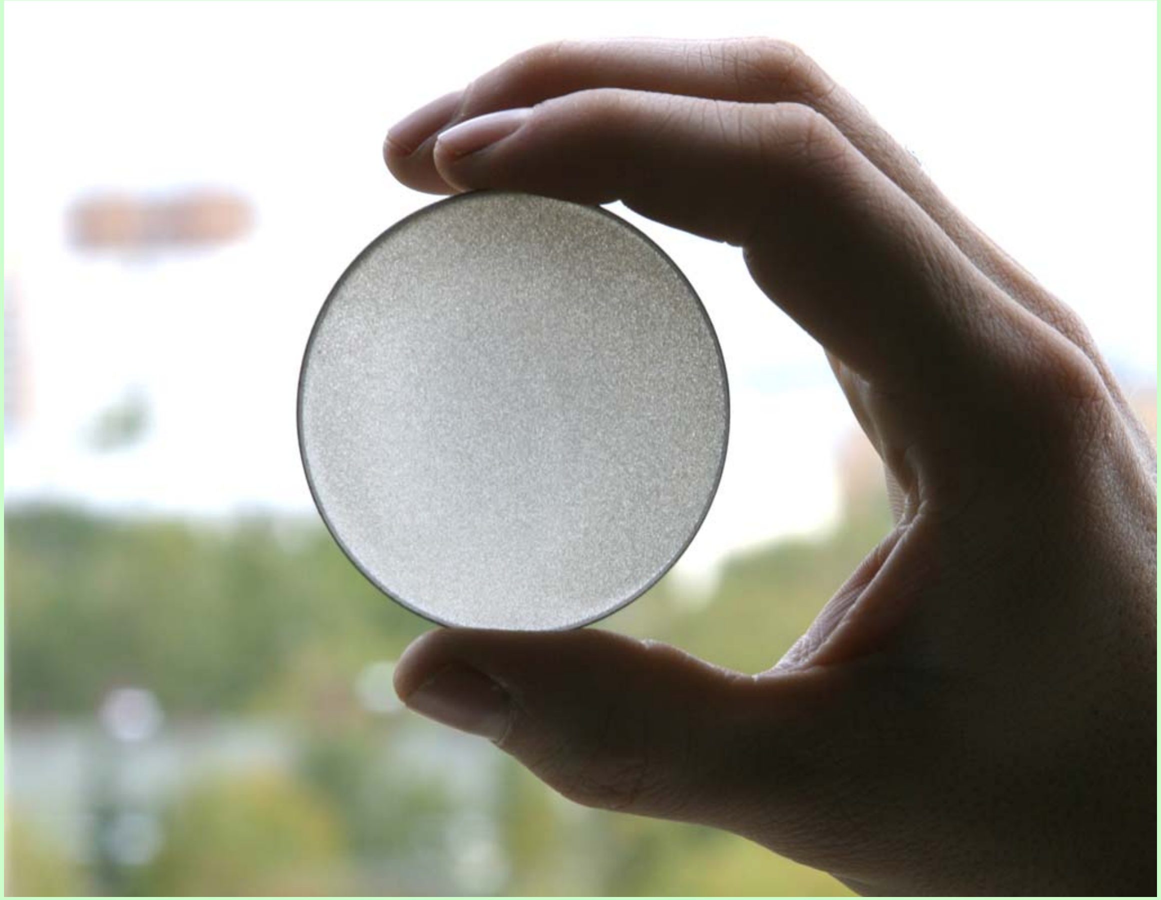

Chemical Vapor Deposition of Diamond

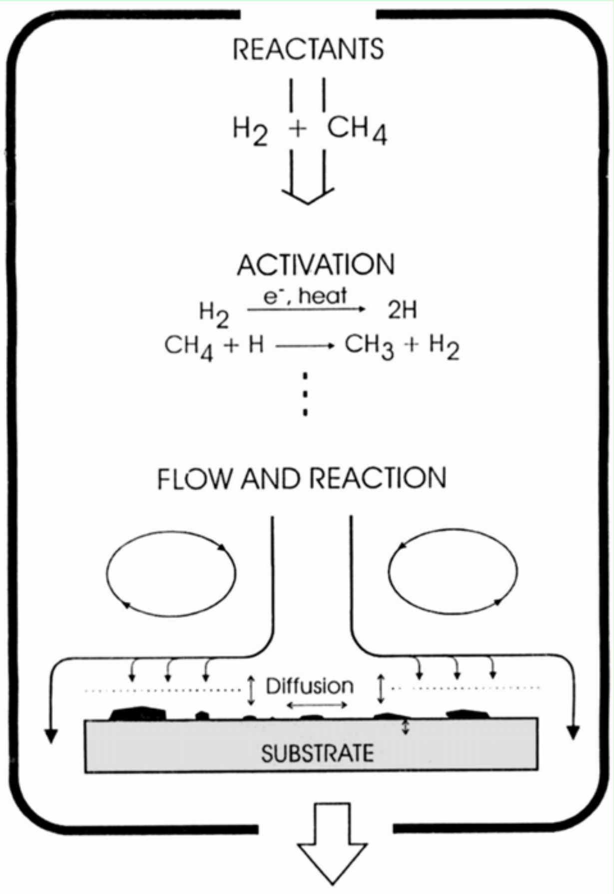

Methods of gas activation

- Hot filament
- DC arc jet
- DC plasma
- Laser plasma
- Oxygen-acetylene flame
- Microwave plasma

Microwave plasma parameters

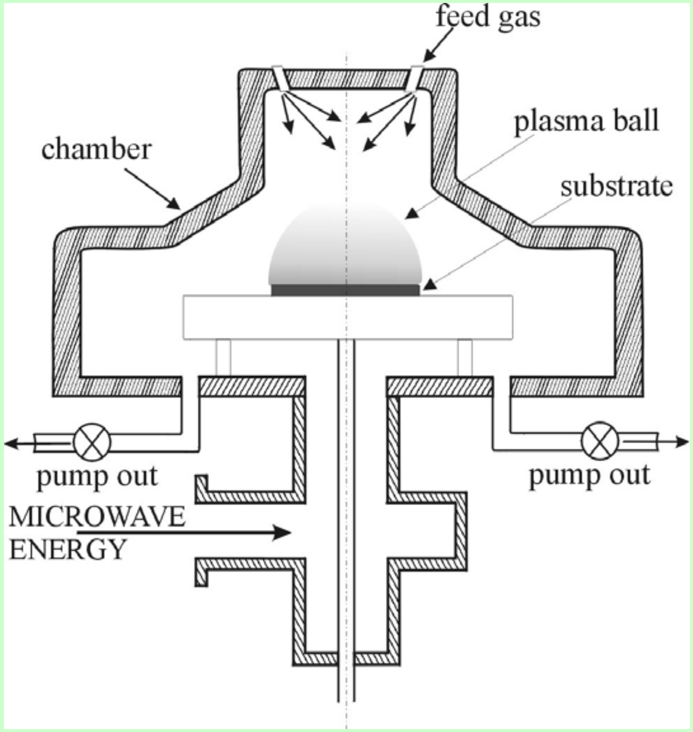

Important for diamond growth:
-high atomic H conc.
-methyl CH_3 radicals

For pure hydrogen plasma, 5.0 kW, 100 Torr:

Neutral gas temperature *Tg*: ca. 2800K from Doppler broadening of Hα line in Balmer series
Electron density *ne*: 1.6×10^{12} cm^{-3} from microwave interferometry at λ=0.8 cm

S. Gritsinin et al., J. Phys. D: Appl. Phys. 31 (1998) 2942.

MPCVD diamond deposition system

DF-100 model, 5 kW, 2.45 GHz

Polycrystalline films

Growth conditions

Gas composition: (1-5%)CH_4/H_2
Pressure: 100 Torr
Flow rate: 1000 sccm
Substrate temperature: 700-900ºC
Substrate diameter: 76 mm (thick films)
100 mm (thin films)
Growth rate: 1-9 μm/hour

Selection of CVD diamond wafers and components

max. diameter 100 mm

Surface texture

grain orientation <110>

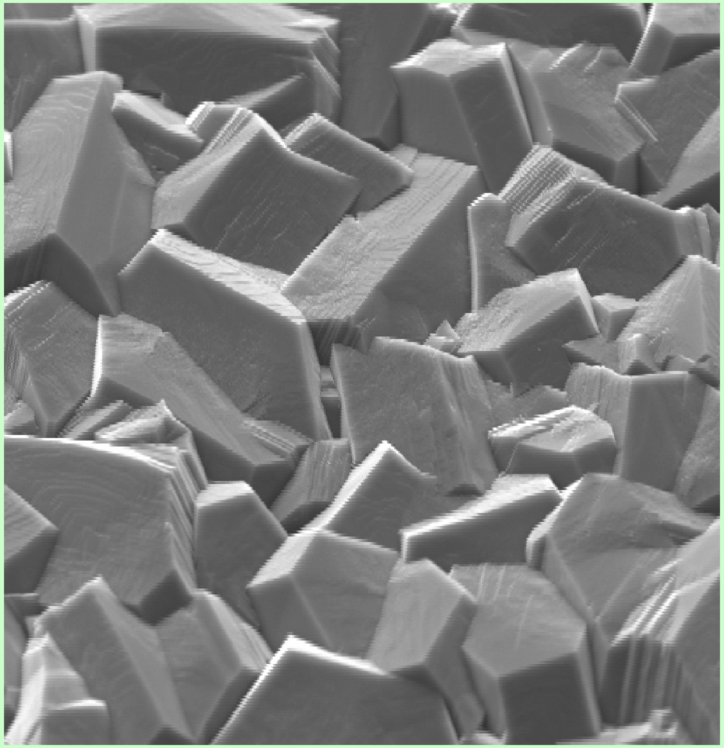

grain orientation <100>

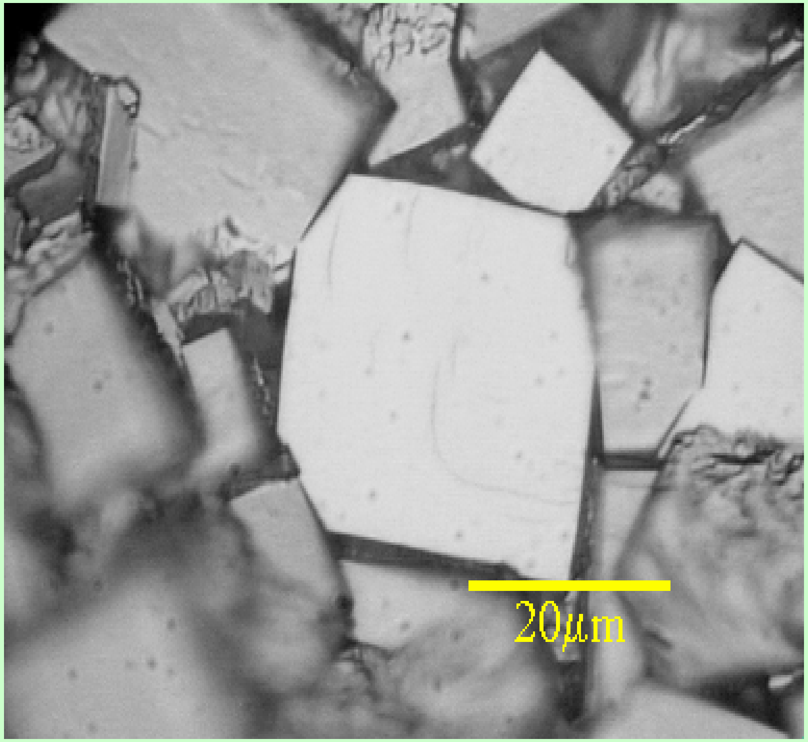

Defects in CVD diamond

TEM study

“white” diamond

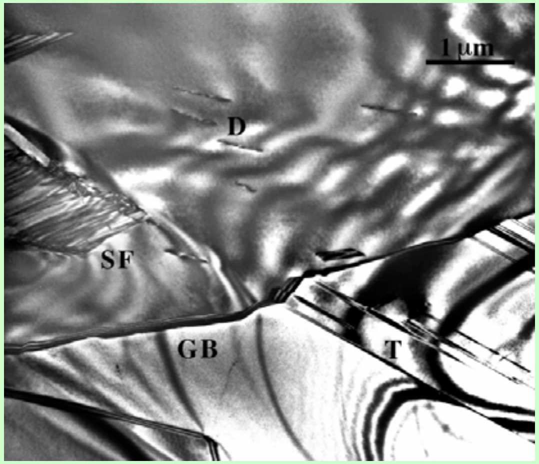

GB - grain boundaries
T – twins
SF – stacking faults
D - dislocations

“black” diamond

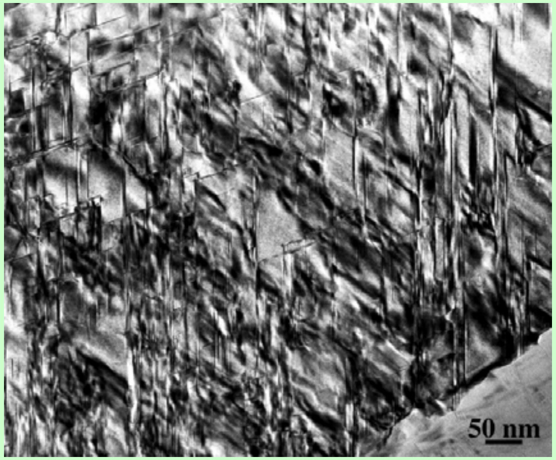

twin bands along <111>

“black” diamond

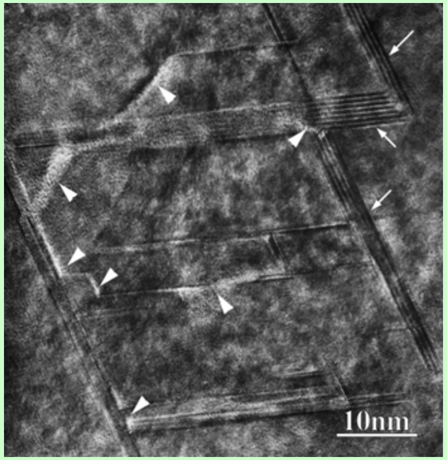

twin intersections, amorphous regions
(atomic resolution)

Raman spectroscopy

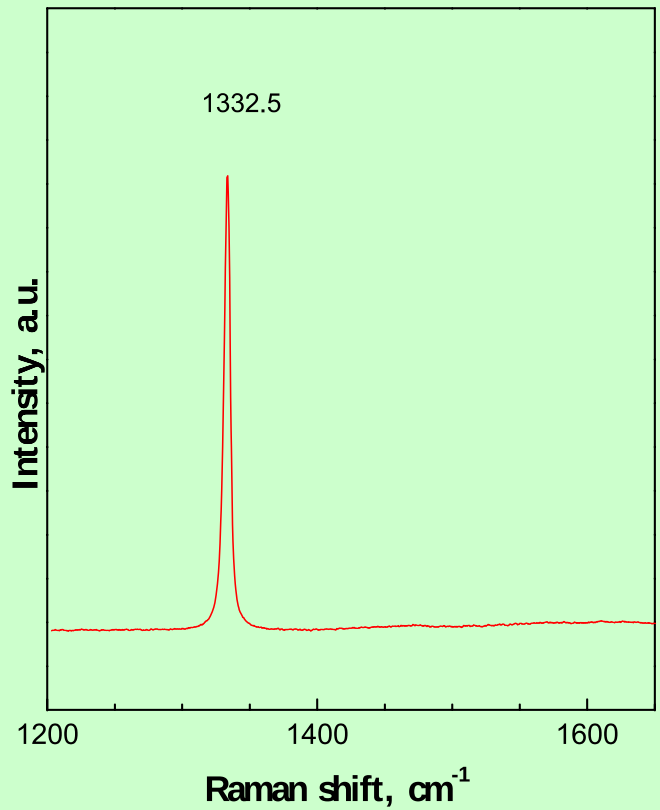

Excitation wavelength 514.5 nm. Peak width 2.2 cm^{-1}.

Optical transmission

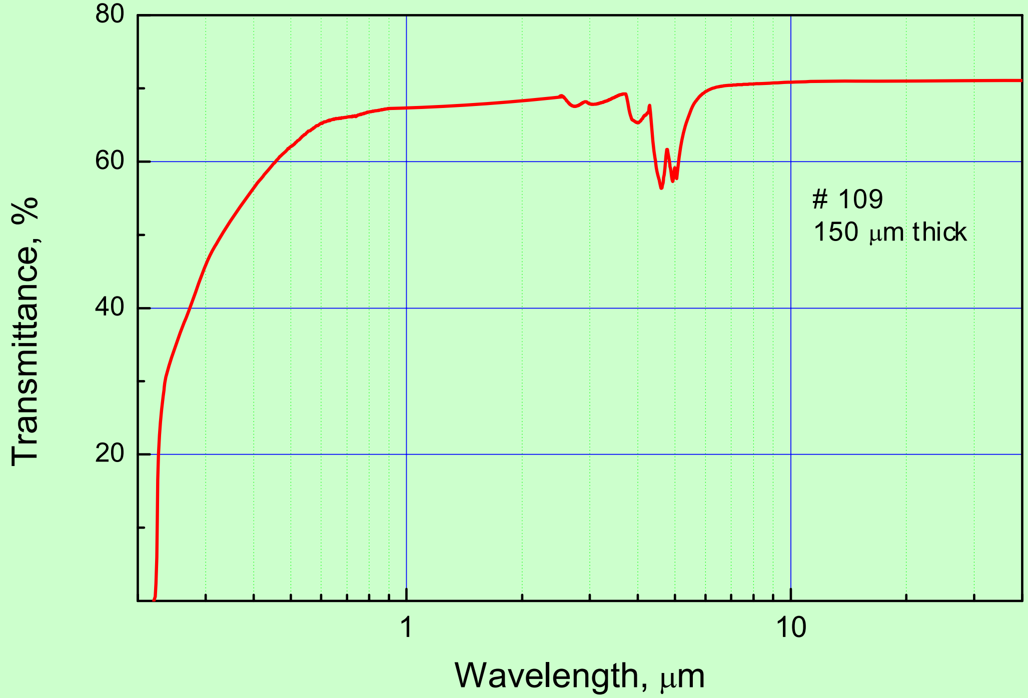

- Cut-off wavelength 225 nm.
- 2-phonon absorption band at 2.5- 6.3 µm is the only intrinsic absorption feature.
- Transparent up to radio frequencies.

Nitrogen and hydrogen impurities in CVD diamond

N and H content evaluation from optical absorption spectra

N-induced UV absorption
270 nm

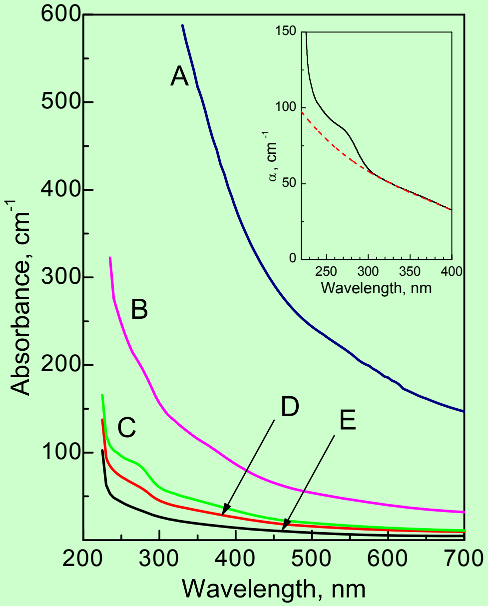

C-H stretch absorption bands
2800-3100 cm^{-1}

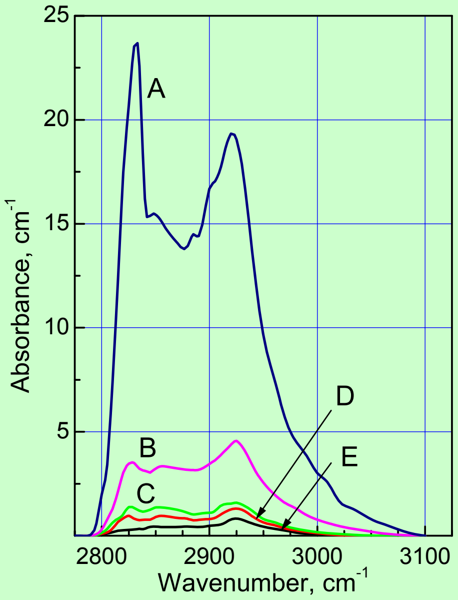

Diamond samples of different qualities A - E

S. Nistor et al. *J. Appl. Phys.* 87 (2000) 8741.

Correlation of (bonded) H and N impurities in MPCVD diamond films

Hydrogen and nitrogen concentrations are determined from IR and UV absorption

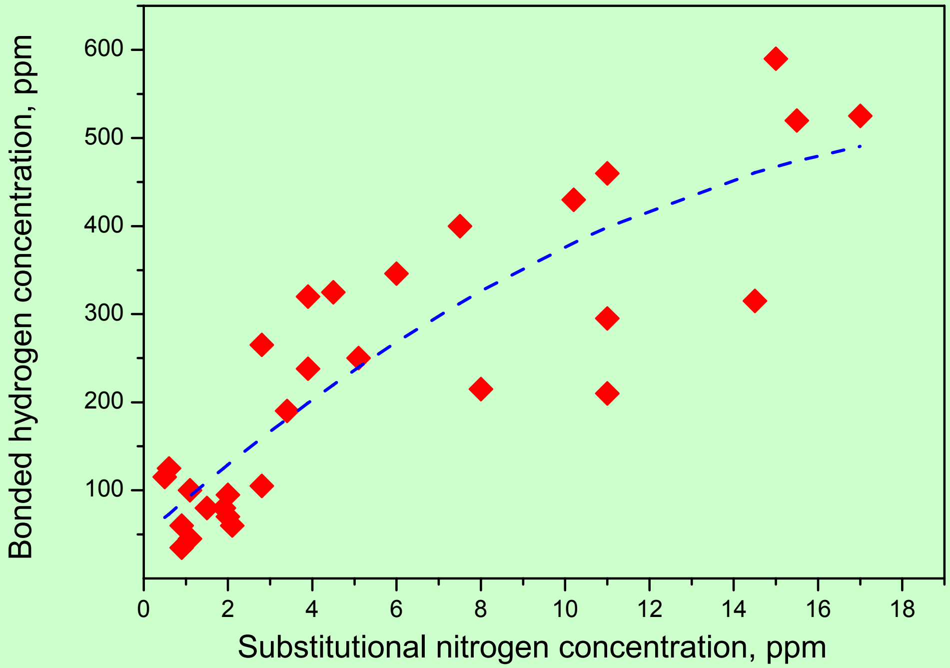

V. Ralchenko, et al. in Hydrogen Materials Science and Chemistry of Metal Hydrides, Kluwer, 2002, p. 203.

Anisotropy of thermal conductivity in polycrystalline CVD diamond

Phonon scattering on grain boundaries.
Columnar grain structure $\Rightarrow$ TC anisotropy.
Depth inhomogeneity due to crystal size variation.

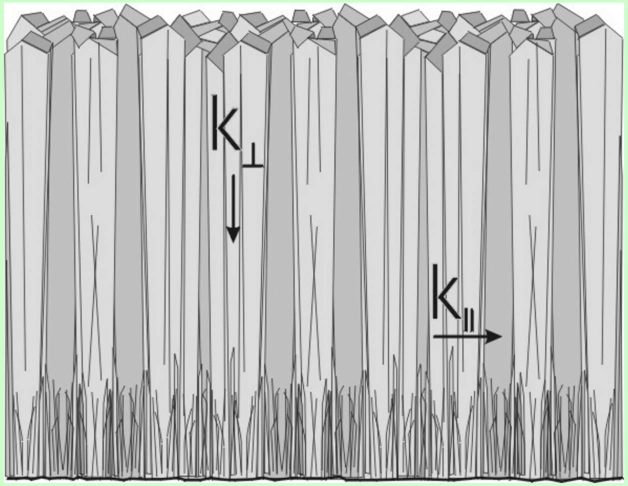

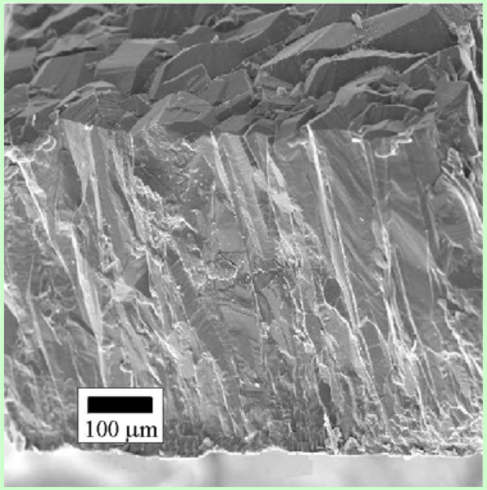

Perpendicular values $k_\perp$ are systematically higher by 10-15% than in-plane values $k_{||}$.

Laser Flash Technique

measures perpendicular thermal conductivity *D*⊥

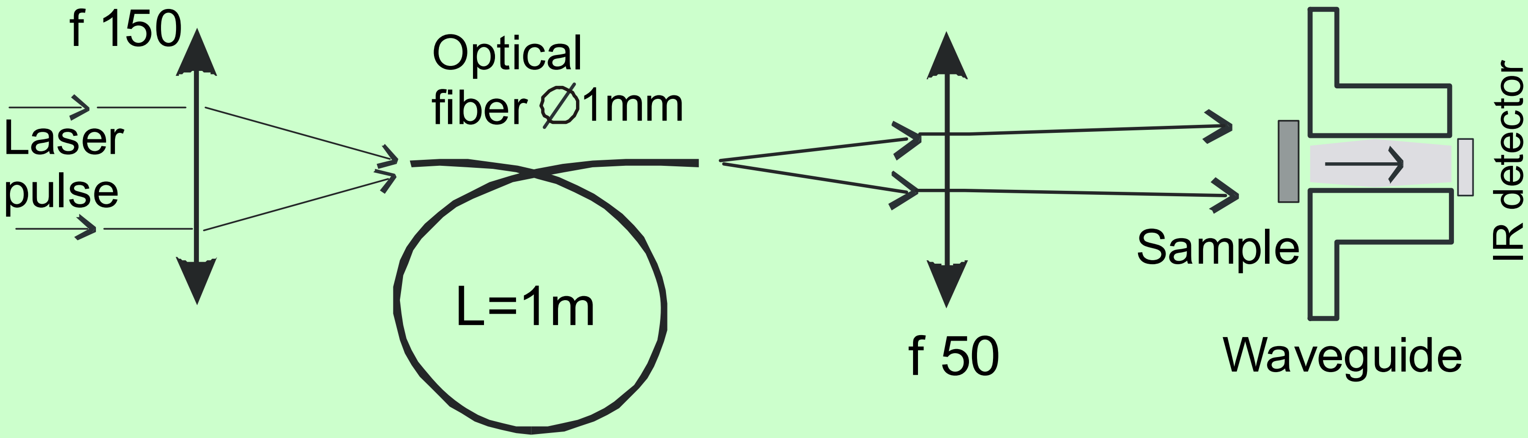

YAG:Nd laser: wavelength 1.06 μm, pulse width 8 ns

HgCdTe detector: 300 ns resolution

V.G. Ralchenko et al., Proc. ADC/FCT 2003, p. 309

Стенд для измерения теплопроводности полиалмаза лазерным флэш-методом

ИАГ:Nd лазер (λ=1,06 мкм, длительность импульса τ=8нс).
КРТ приемник теплового ИК излучения

Laser Flash Technique

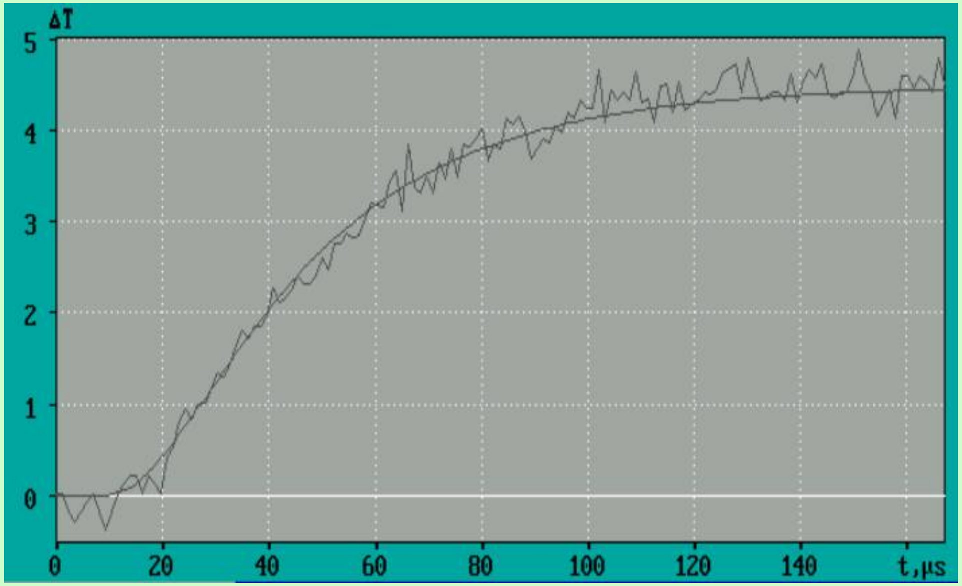

- Assume:
  one-dimensional heat flow
- Measure:
  $\Delta T(t)$ on the rear side of diamond plate

Approximation: $T(t) = Q/d\ C\ \{1+2\sum(-1)^n \exp(-n^2\pi^2 D_\perp t/d^2)\}$

D is film thickness, Q-pulse energy, C is heat capacity

Thermal diffusivity $D_\perp = 1.38 d^2/\pi^2 t_{1/2}$

Thermal conductivity $k_\perp = \rho C D_\perp$

Transient thermal grating technique

measures parallel thermal *diffusivity* $k_{||}$

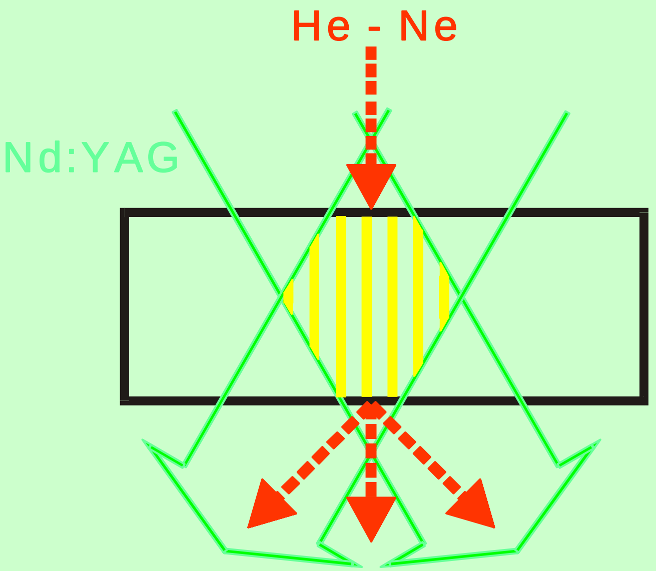

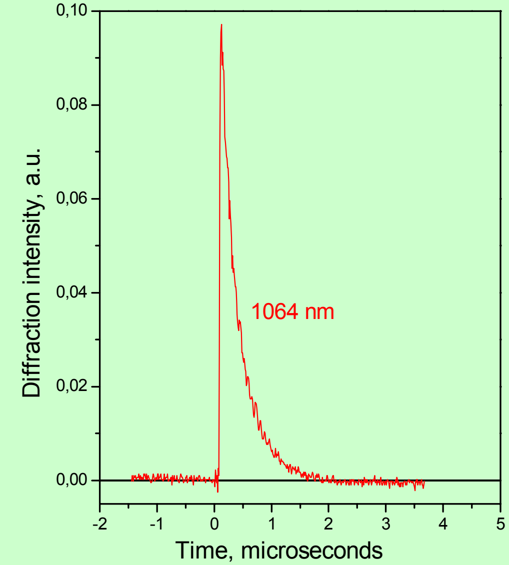

- thermal grating formation due to refraction coefficient modulation by two interfering laser (Nd:YAG) beams

- diffraction of probe He-Ne laser beam on the transient grating with period Λ

Diffraction signal decay due to thermal dissipation

$$\tau = \frac{\Lambda^2}{4\pi^2 D_{II}}$$

Anisotropy of thermal conductivity in polycrystalline CVD diamond

Phonon scattering on grain boundaries.
Columnar grain structure $\Rightarrow$ TC anisotropy.
Depth inhomogeneity due to crystal size variation.

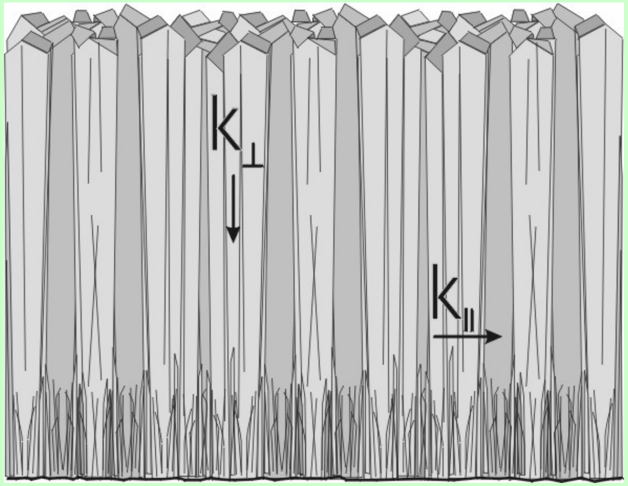

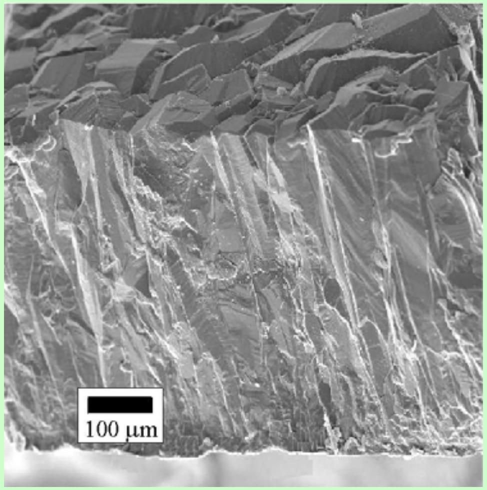

Perpendicular values $k_{\perp}$ are systematically higher by 10-15% than in-plane values $k_{||}$.

Thermal conductivity at room temperature

sensitive to hydrogen impurity content

- Bonded hydrogen (C-H) decorates defects and grain boundaries.
- Hydrogen concentration as an indicator the defect abundance in CVD diamond.

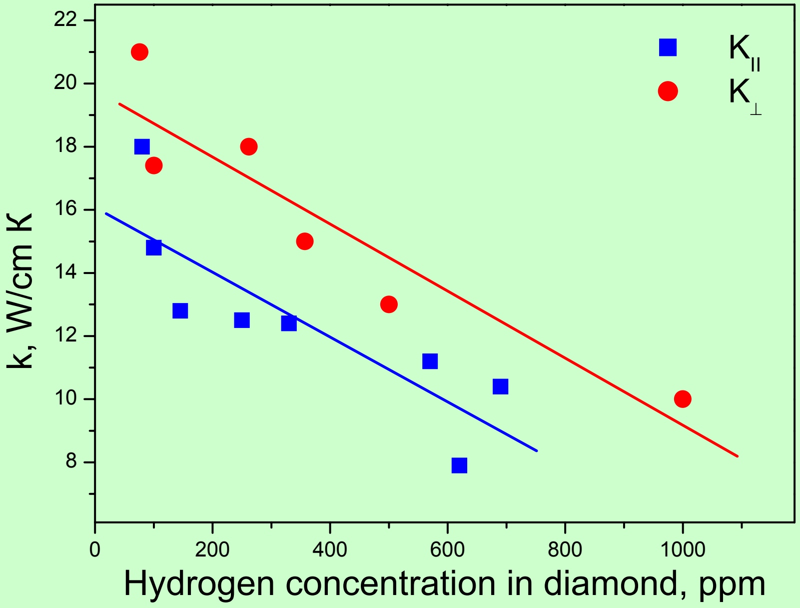

Perpendicular values $k_{\perp}$ are systematically higher by 10-15% than the in-plane values $k_{||}$.

Thermal conductivity at elevated temperatures
T = 293-460 K

Thermal conductivity decreases with T due to phonon-phonon scattering.
Approximation $k \sim T^{-n}$

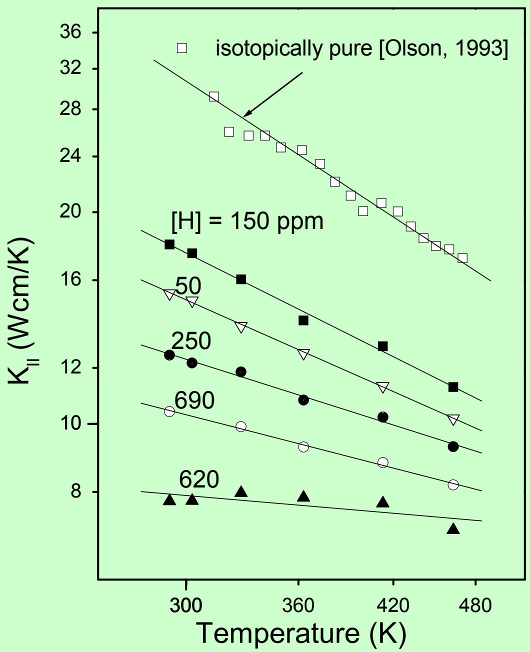

Concentration of H impurity (in ppm) is indicated for each sample.

The data for isotopically pure (^{12}C) synthetic HPHT single crystal diamond [Olson PB'1993] give n=1.36, the highest slope for any diamond.

Exponent n = 0.17 – 1.02 increases with diamond quality

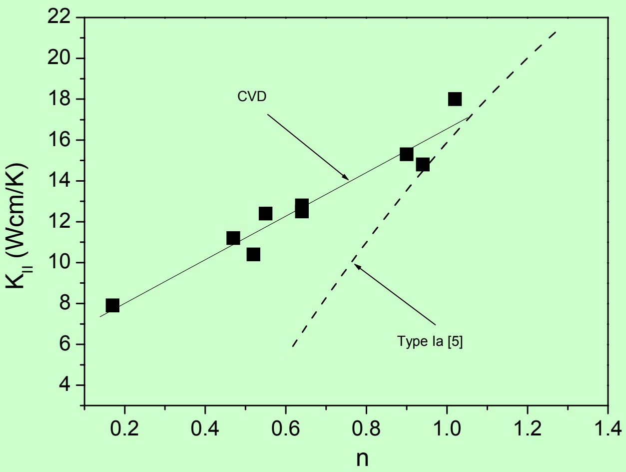

● Comparison with data for single crystal *natural* diamonds [Burgemeister, Physica, 1978].

● Weak temperature dependence for highly defective CVD diamond.

Thermal stability of CVD diamond

vacuum annealing for 1 h

- Stability of optical absorption up to 1200ºC.
- Darkening at higher temperatures. Break at 1700^{o}C.
- More defective samples degrade easier.

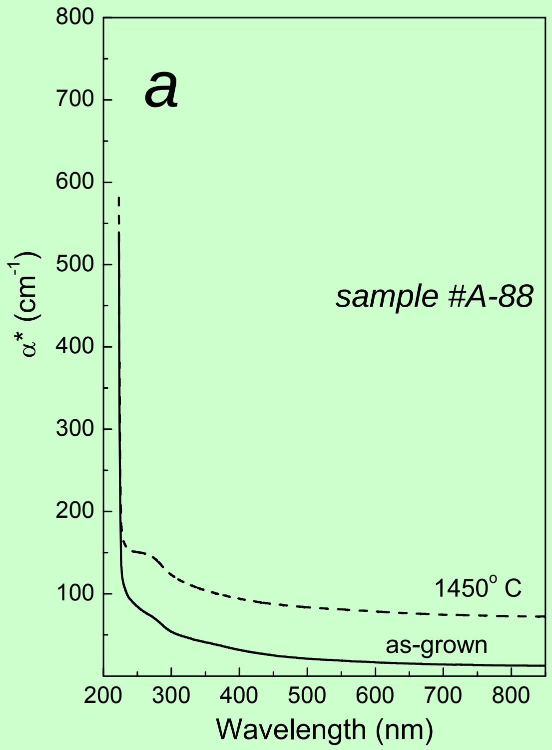

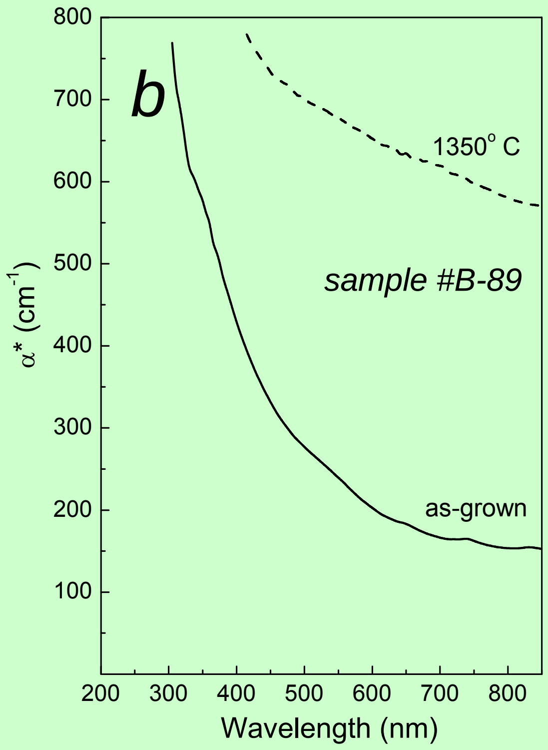

V. Ralchenko et al. Diamond Relat. Mater. 12 (2003) 1964 .

Graphitization of grain boundaries

vacuum annealing at 1450ºC for 1 hour

junction of three GBs

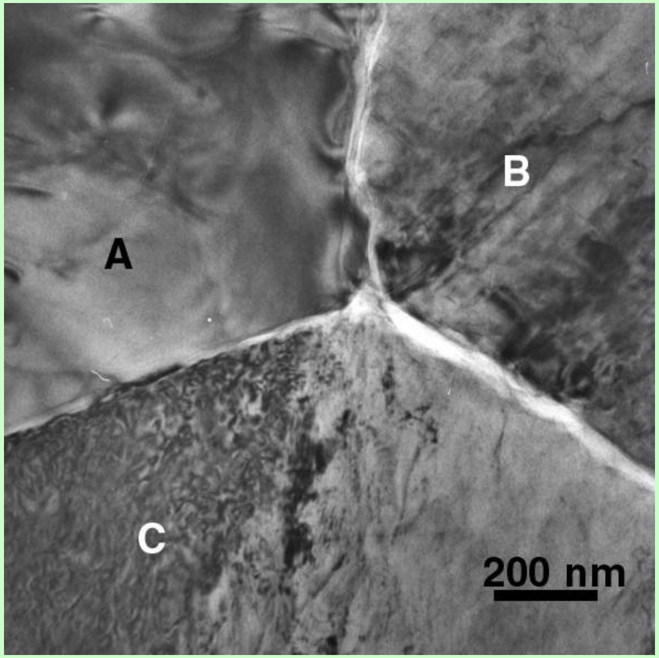

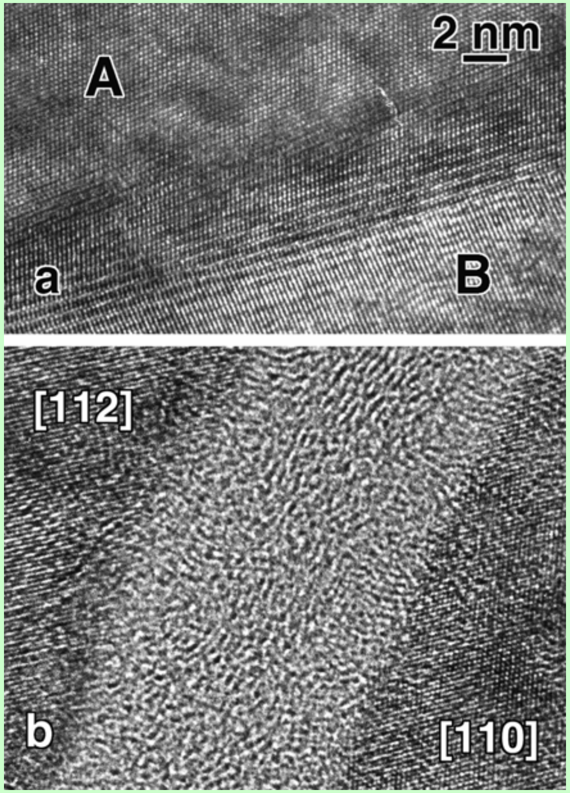

L. Nistor et al. Phys. Stat. Sol. (a), Vol. 186, No.2 (2001) 207

Graphitization of internal (structural) defects
vacuum annealing

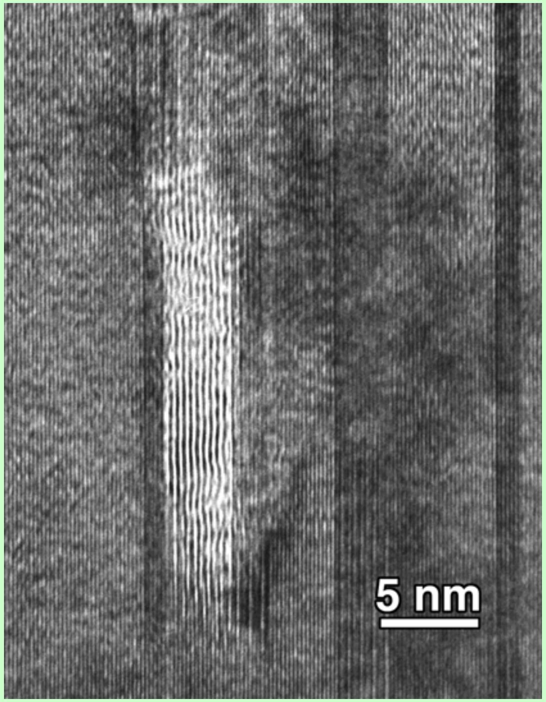

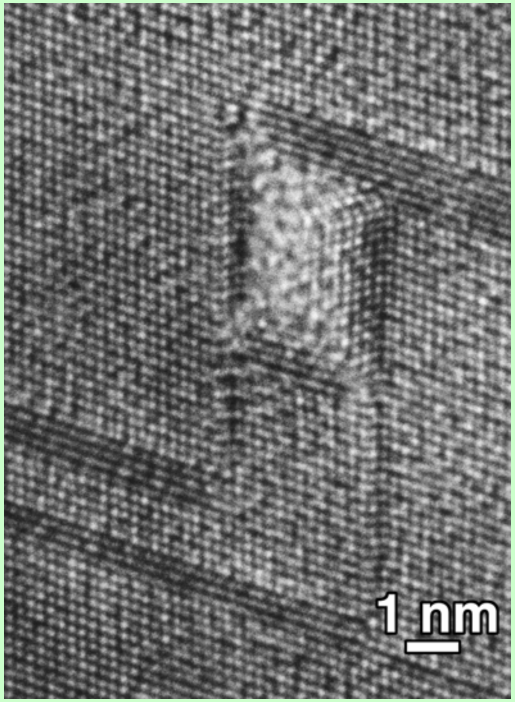

- Graphitic domains inside the grain.
- Three (111) diamond planes transform to two (0002) graphite sheets.
  Minimization of interface strain energy.

Abrasive polishing

CVD-diamond of 0.5 mm thickness. Edges are laser cut.

as-grown surface

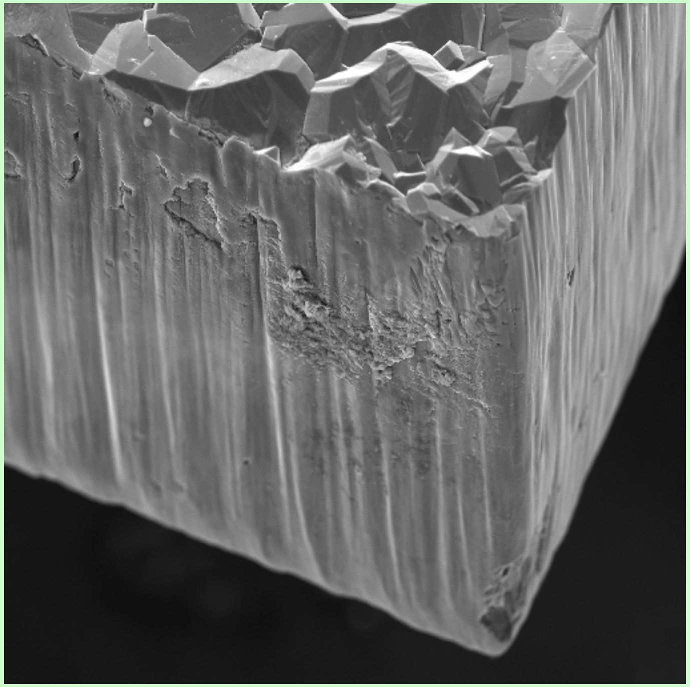

polished surface

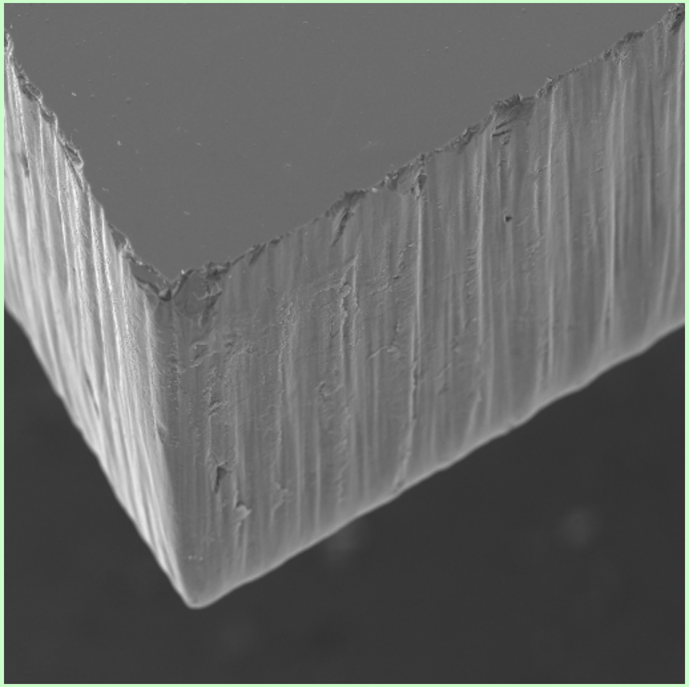

Surface roughness Ra<10 nm
(Ra<1 nm within single grain)

Laser treatments

polishing

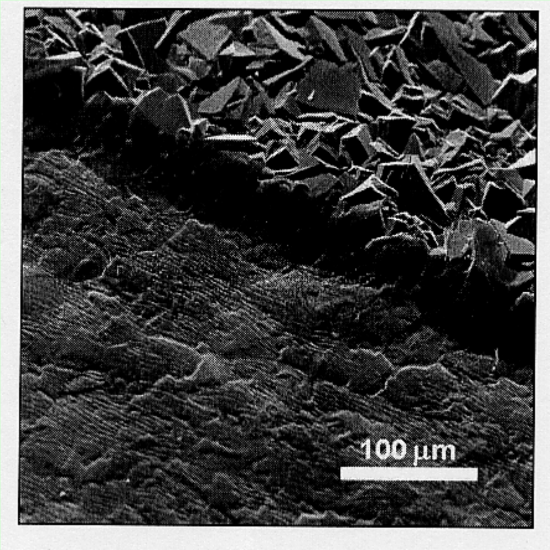

KrF excimer laser

drilling

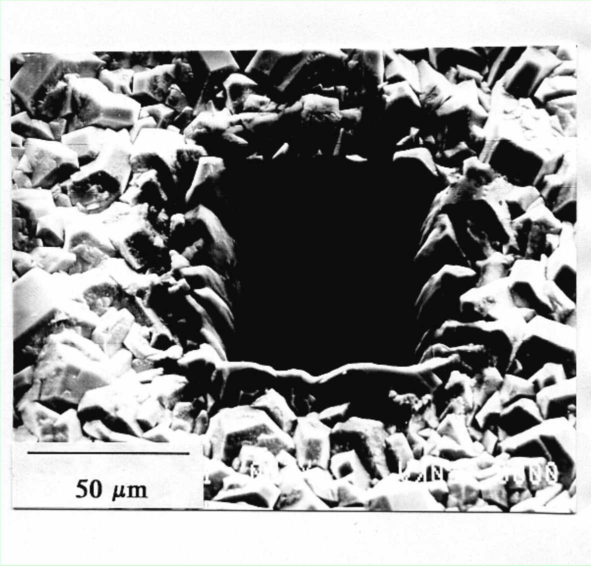

Copper vapor laser

cutting

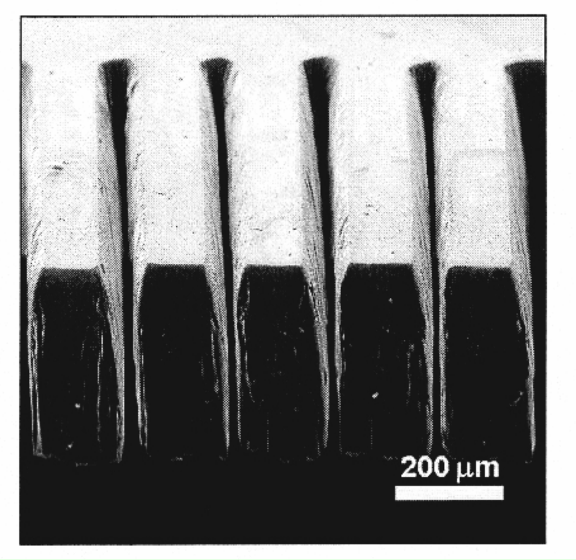

Nd:YAG laser

Doping of diamond

p-type conductivity

acceptor	activation energy E_a, eV
B	0.37
H (surface only)	0.05

n-type conductivity

donor	Ea, eV
N	1.7
P	0.6

All impurity levels (except hydrogenated surfaces) are deep.
Compare with B-doped Si in which E_a = 0.046 eV.

Properties of Si and diamond important for detector applications

at room temperature

material	Si	diamond
proton number, Z	14	6
mass density, g/cm^3	2.33	3.5
band gap, eV	1.12	5.47
breakdown field, V/µm	30	1000
saturation velocity, µm/ps	0.1	0.27
energy ε_{pair} to create *eh*-pair, eV	3.6	13
specific ionization loss ε_{loss}, eV/mm	0.321	0.469
av. no. of *eh*-pairs/*mip*, e/0.1mm	8900	3600

from D. Meier, CERN, 1996

CVD diamond UV detectors

Solar-blind

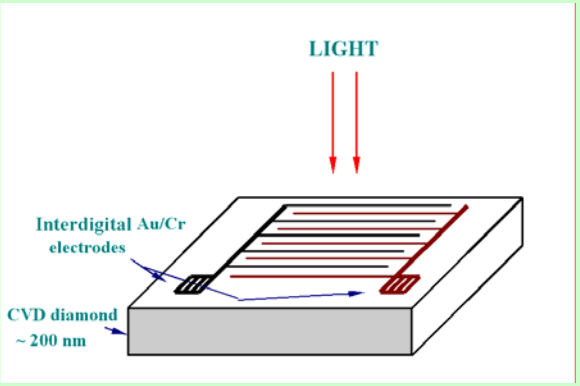

Interdigitizing electrodes on polished diamond. Cr(20 nm)/Au(500nm) strips 50 μm wide, the gap between electrodes is 50 μm.

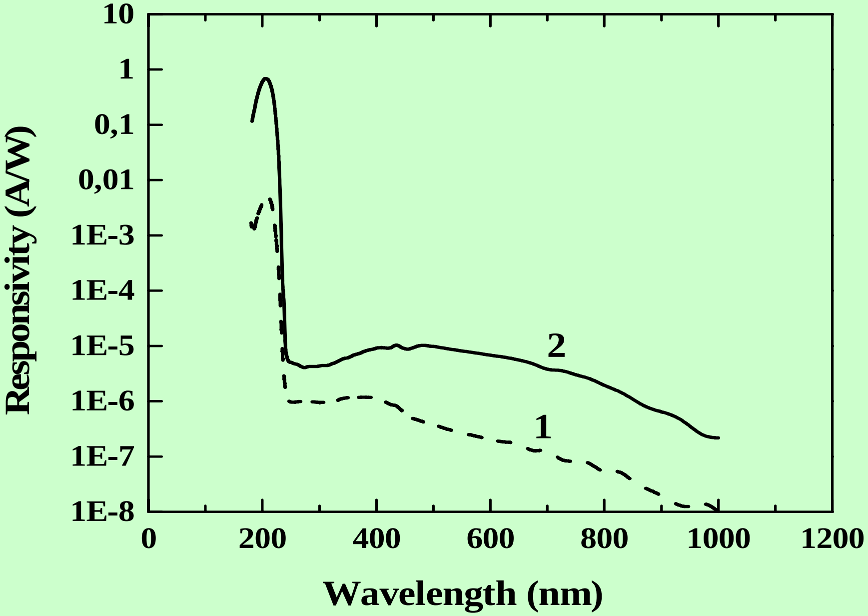

Spectral discrimination UV/Vis of 10^5.
Dark current of the order of 1 pA.

Particle detector

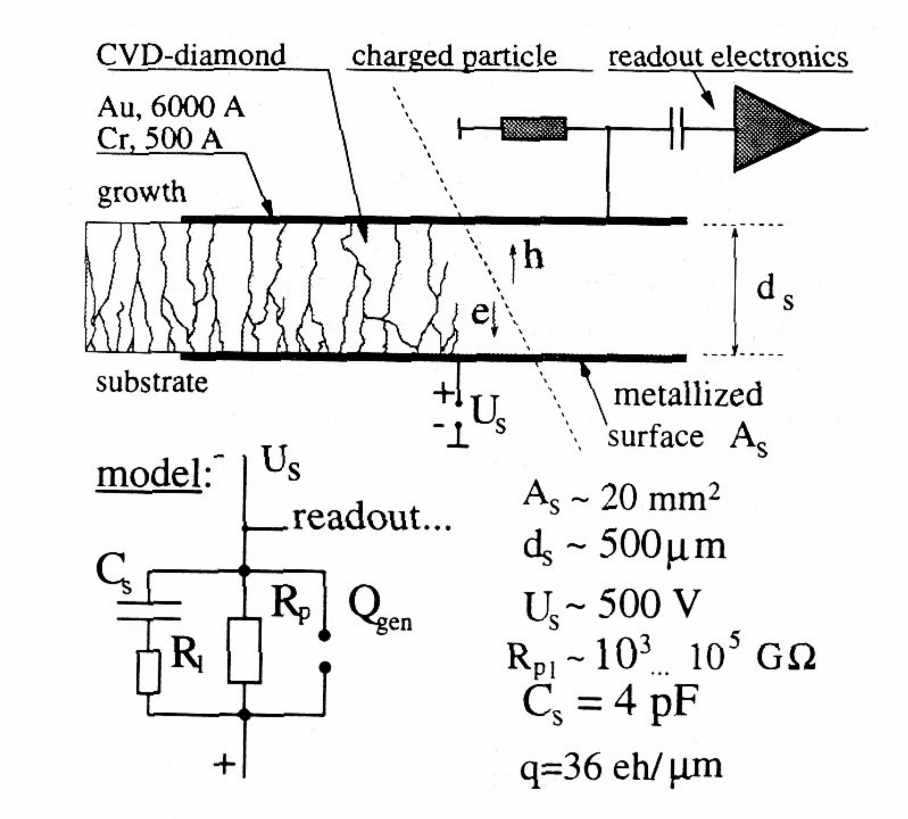

from D. Meier, RD42 Collaboration, 1996

Charge collection distance

$d = \mu\tau E$

RD42 Collaboration data for
De Beers CVD diamond samples:

d = 200 µm (year 2000)

$d_{max} \approx 300\ \mu m$

Stable up to dose ~10^{15} cm^{-2}
under protons, neutrons, pions.

Electron mobility-lifetime products for detector materials in nuclear applications

"Detector-grade" material	Mobility-lifetime product for electrons ($\mu\tau$) (cm^2/V)
Si	1
CdTe	10^{-3}
SiC	$10^{-4} - 10^{-5}$
GaAs	10^{-6}
CVD diamond *polycrystalline* *single crystal*	10^{-6} 10^{-4}

from C. Manfredotti, *DRM* 14 (2005) 531.

Single crystal CVD diamond

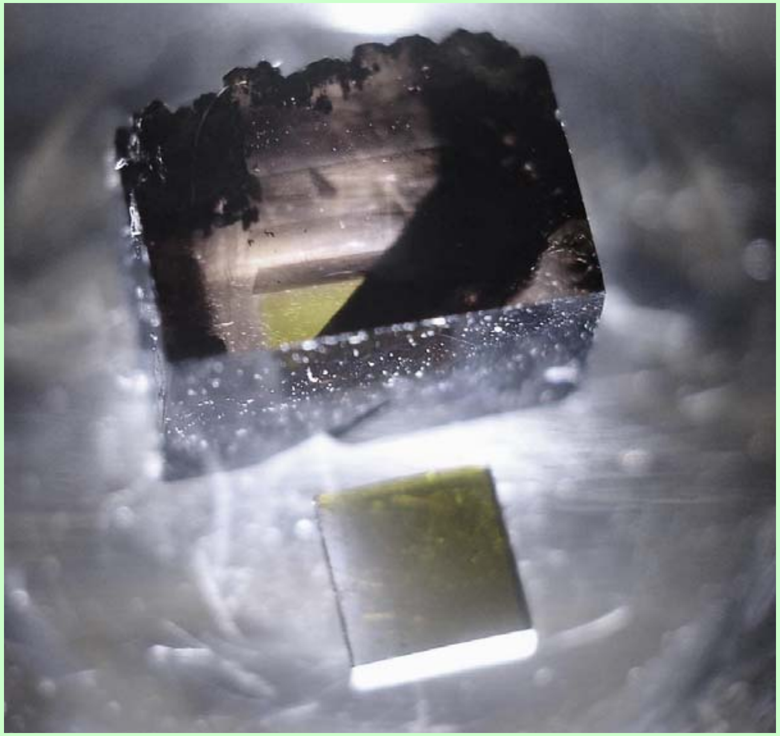

Carnegie Institute, Washington (2002)
Substrate: HPHT single crystal diamond
Diamond deposition: microwave plasma CVD
Growth rate: up to 150 μm/hour
Max size: 10x10x10 mm (year 2005)

Charge collection distance
d = 420 μm (year 2003)
measured by RD Collaboration

Single-crystal diamond block formed by deposition on 6 {100} faces
of a substrate diamond, such as the 4 x 4 x 1.5 mm^3 crystal shown below.

Neutron sensors

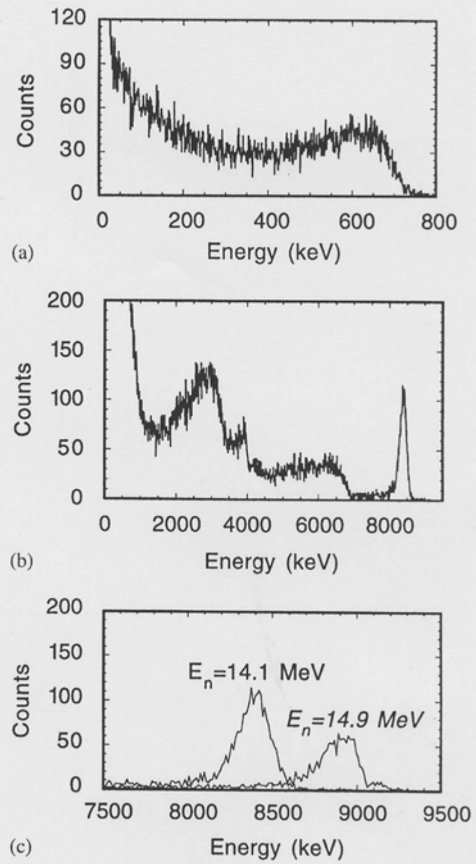

Fig. 7. Counts vs. energy deposited in single crystal CVD diamond sensor for incident neutrons of energy (a) 2.5 MeV, (b) 14.1 MeV, and (c) 14.1 and 14.9 MeV (expanded view showing the (n, α) peaks). The spectra have been calibrated based on known endpoint energies: 700 keV for the 2.5 MeV neutrons, and 8.4 MeV for the 14.1 MeV neutrons. All data at +100 V bias.

Energy resolution for 14 MeV neutrons:

Best natural diamond ≈2%

M. Pillon et al. NIM B101 (1995) 473

← Single crystal CVD diamond <2.9%

G. Schmid et al. NIM A527 (2004) 554

On-line diamond X-ray detector

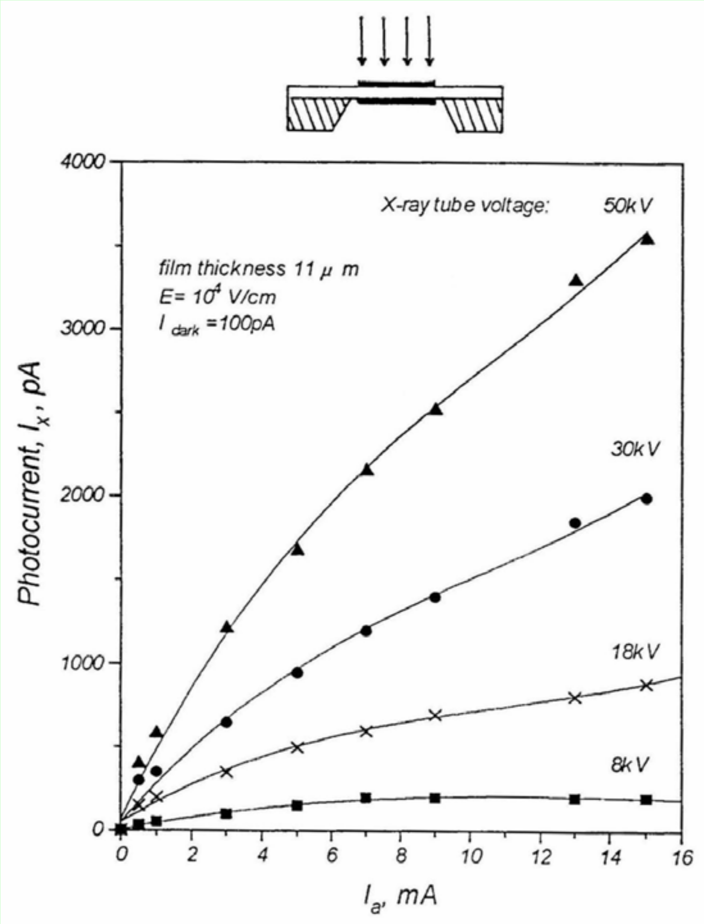

Diamond membrane: 10 μm thickness, window of 7 mm diameter.

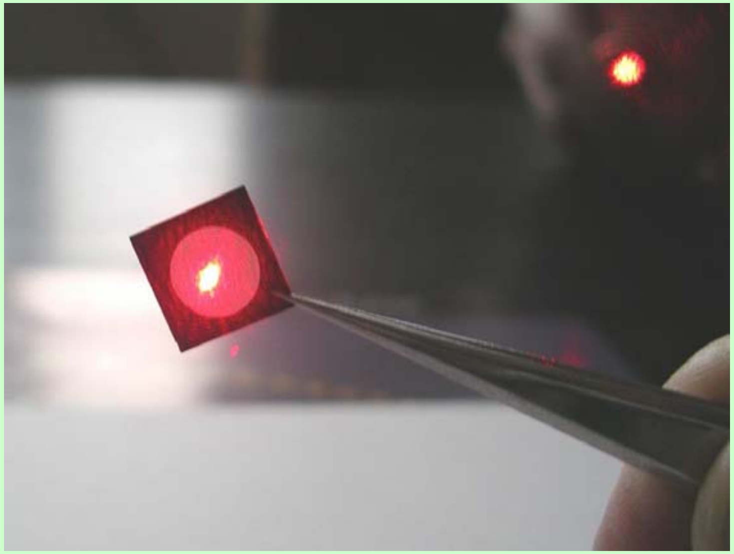

X-ray transmission (50 keV) > 98%.

Source: X-ray tube with tungsten anode.
Photocurrent/dark-current ratio: $8x10^3$ at U_a=50 kV.
V. Dvoryankin et al. (1998).

Polycrystalline CVD diamond field effect transistor (MEDFET) on H-terminated diamond surface

Hydrogenated diamond surface shows p-type conductivity with low (ca. 50 meV) activation energy

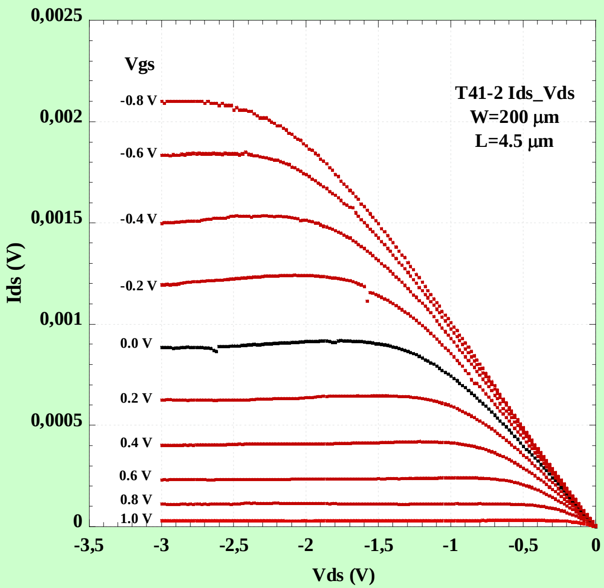

Output characteristic of a MEDFET with channel length L=4.5 µm

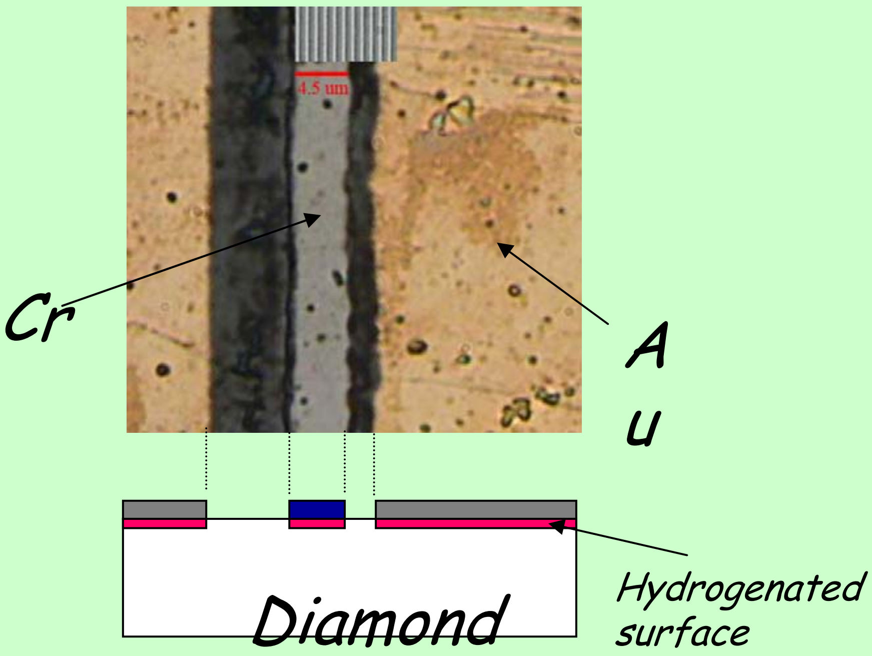

G. Conte et al, 2005 (unpublished)

Gyrotrons – generators of powerful *mm* waves (~100-200 GHz)

Requirements to gyrotron window material:

- very low absorption (low loss tangent)
- low dielectric permittivity, ε.
- high thermal conductivity, k,
- high mechanical strength (Young's modulus, E)
- low thermal expansion coefficient, α

Properties of some materials important for mm-waves windows

(T=293 K and f=145 GHz)

Material	ε	tanδ (10^{-4})	k W/cmK	α 10^{-6} K^{-1}	E GPa
Fused quartz	**3.8**	**3**	**0.014**	**0.5**	**73**
BN	**4.3**	**5**	**0.35**	**3**	**60**
BeO	**6.7**	**10**	**2.5**	**7.6**	**350**
Sapphire	**9.4**	**2**	**0.4**	**8.2**	**380**
Au-doped Si	**11.7**	**0.03**	**1.4**	**2.5**	**160**
Diamond	**5.7**	**0.08* 0.03****	**20**	**0.8**	**1050**

*Diagascrown/GPI sample [B. Garin et al. *Techn. Phys. Lett*. 25 (1999) 288]

**DeBeers sample [V. Parshin et al. *Proc. 10th Int. ITG-Conf. on Displays and Vacuum Electronics*, 2004]

Vacuum-tight CVD diamond window

brazed to copper cuffs

Window diameter 60 mm and 15 mm

TEST

Thermal cycling:

- 25-750-25°C and (–60)-(+150)°C
- 8 hours heating at 650°C.

Result: no degradation in vacuum tightness.

Molding technique

Avoid post-growth treatment. Net-shape growth approach.

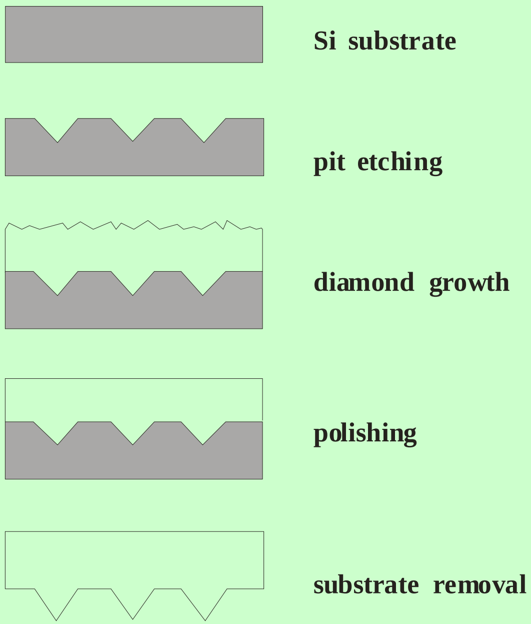

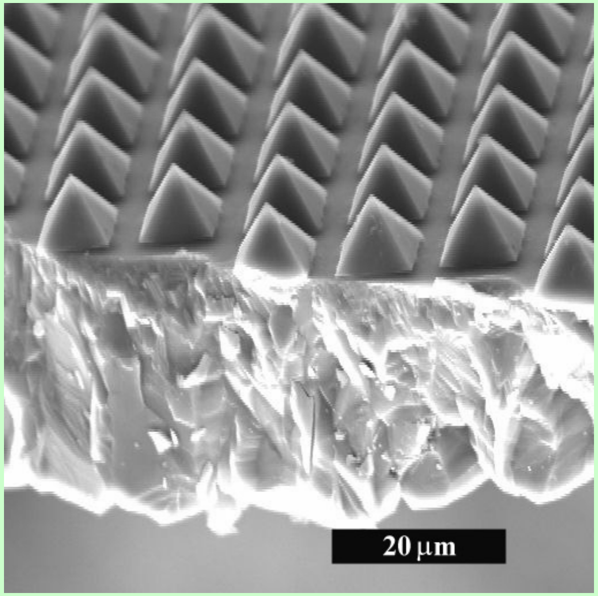

Diamond pyramids
9 μm base length, 12 μm period

Optical transmission spectra of ARS diamond surfaces

Pyramids with period Λ=4.5 μm and Λ=12 μm

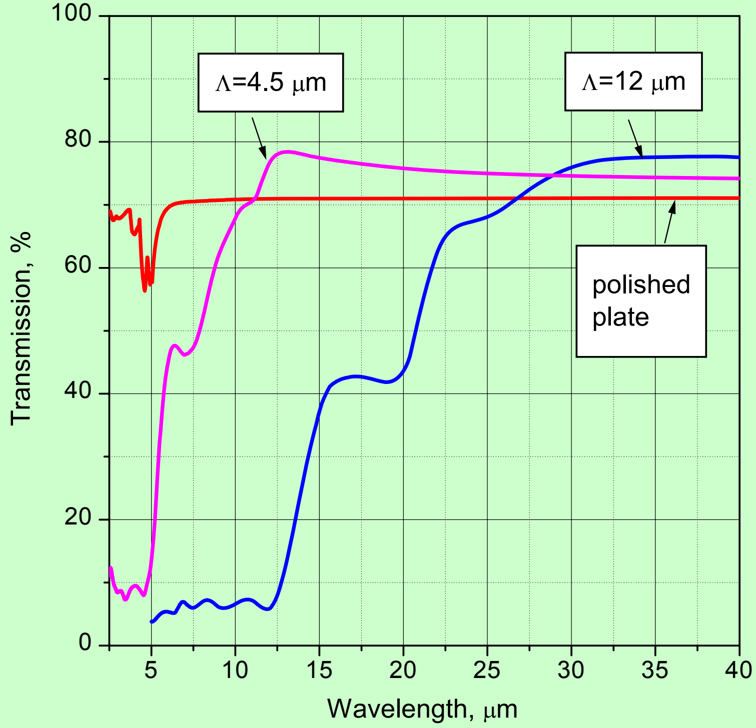

- ARS as a gradient effective refraction index layer.
- Enhanced transmission of ARS surface occurs at Λ>10.8 μm and Λ>10.8 μm for small and big pyramids, respectively.
- ARS critical periods: for λ = 10.6 μm (CO_2 laser) Λ = λ/n=4.4 μm;
  for λ = 2 mm (gyrotrons) Λ = 0.83 mm

X-ray refractive diamond lenses produced by molding technique

A. Snigirev et al. SPIE Proc. 4783 (2002) 1.

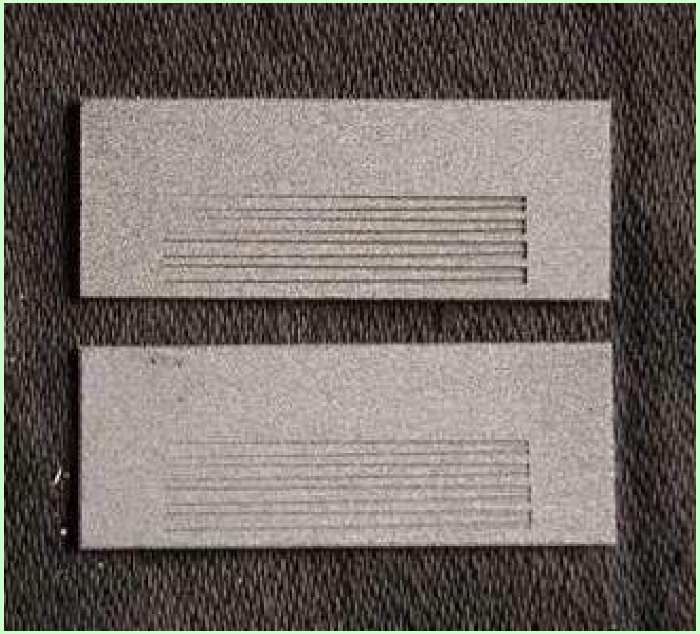

15 x 40 mm^2 diamond plates with relief depth of 100 and 200 μm. Four parabolic lenses are formed on each 110 μm thick plate.

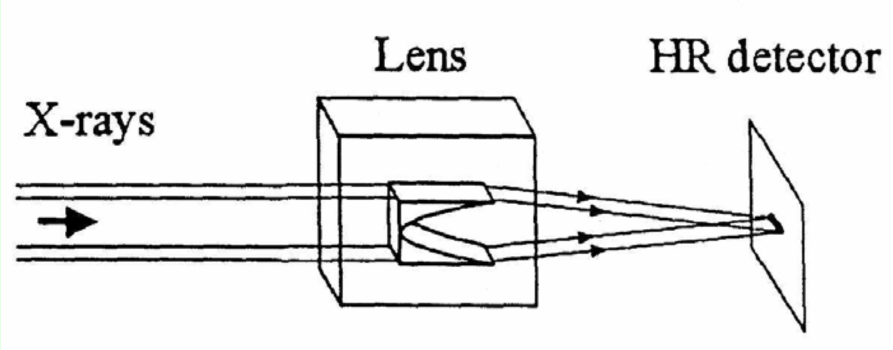

Tests at synchrotron in Grenoble

- The beam focusing to 2.2 μm spot size at the focal distance of 0.5 m with T=25% transmission at photon energy 9 keV, and T=80% at 38 keV.
- Lens gain: 22-100.
- Stable performance at the beam power density 50 W/mm^2.

Integrated Diamond Tip and Cantilever for Scanning Force Microscopy

* cantilever is cut by a Nd:YAG laser
* tip with 100 μm base length is grown by a molding technique

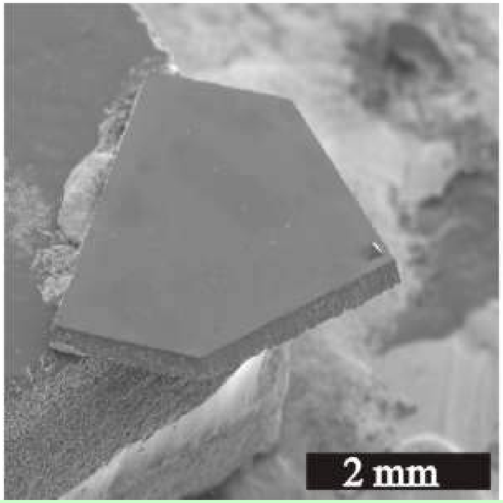

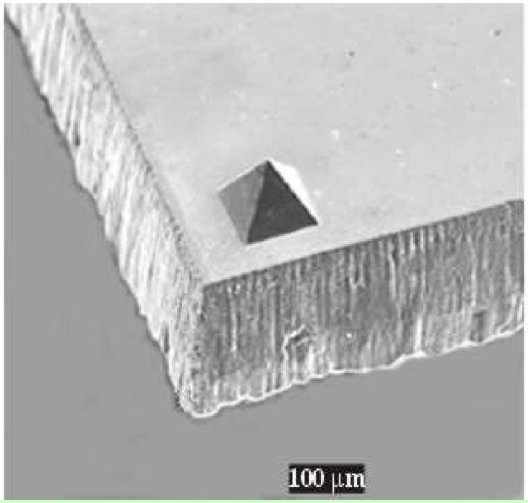

Conclusions

● Polycrystalline diamond films (and, recently, single crystals) of high purity and large size can be produced by CVD technique.

● The properties of CVD diamond approach (in some cases exceed) those known for the best natural single crystal diamonds.

● Potential application of the CVD diamond include, in particular:
-- detectors of ionizing radiation;
-- IR and microwave optics for CO2 lasers, gyrotrons, etc;
-- radiation-hard, high-temperature electronics;
-- cutting tools;
-- GHz-range devices based on surface acoustics waves;
-- new applications…